Journal of New Materials for Electrochemical Systems 15, 165-170 (2012)
© J. New Mat. Electrochem. Systems

Nanostructured Pt/WO$_x$-C Solids as Electrocatalyst for PEMFC

M.L. Hernández-Pichardo[1,*], R.G. González-Huerta[2], P. del Angel[3], E. Palacios-González[3] and S.P. Paredes-Carrera[1]

[1]Instituto Politécnico Nacional-ESIQIE. Laboratorio de Investigación de Fisicoquímica y Materiales, UPALM, 07738, México, D. F.
[2]Instituto Politécnico Nacional -ESIQIE, Laboratorio de Electrocatálisis, UPALM, 07738 D.F. México, D.F.
[3]Instituto Mexicano del Petróleo, Dirección de Investigación y Posgrado, Eje Central L. Cárdenas 152, 07730, México, D. F.

Received: December 14, 2011, Accepted: February 10, 2012, Available online: March 22, 2012

Abstract: *Platinum nanoparticles supported on high surface area carbon black (e.g., Vulcan XC-72) are the most commonly used catalysts for both cathode and anode in proton exchange membrane fuel cells (PEMFCs), however, some other catalysts such as Pt/MoO$_x$ and Pt/WO$_x$ are also considered promising, due to their higher activity, stability and enhanced CO tolerance. This work is focused on the synthesis and characterization of nanostructured Pt/WO$_x$-C as both cathode and anode electrocatalysts for PEMFCs. The Pt deposit on the surface of the support is a crucial step in the synthesis of the catalytic materials. Because of this, different synthesis methods were probed in order to find the conditions for the higher dispersion and accessibility of Platinum over the WO$_x$-C support and to improve the PEMFC cathode stability. The catalysts were prepared by UV and ultrasound assisted approaches, and characterized by Transmission Electron Microscopy as well as lineal and cyclic voltammetry.*

Keywords: Polymer Electrolyte Fuel Cell; Electrocatalyst; Platinum; WO$_x$ nanostructures.

1. INTRODUCTION

Practical catalysts for low-temperature fuel cells are typically in the nano-size range and are typically deposited on high-surface-area supports. The Degradation of the catalyst support material in the cathode of the proton exchange membrane fuel cell (PEMFC) has been discussed recently. Previously some authors have reported on the corrosion of the catalyst-supporting carbon in the context of PEMFC. The cathodic PEMFC environment, including high acidity, electrochemical potential, water content as well as O_2 concentration, sets high demands on the catalyst support material. The presence of Pt on carbon increases significantly the rate of carbon corrosion. The carbon corrosion results in a decreased contact between the support and the Pt catalyst particles, which consequently become more mobile and might form larger Pt aggregates or migrate out of the cathode. Carbon degradation can also cause increased hydrophilicity of the supporting carbon, which results in deteriorated mass-transport properties of the cathode [1,2]. One current approach for eliminating carbon corrosion is to optimize operation conditions, e.g. avoidance of high humidity levels and high-voltage operation. Another approach is the development of more stable supporting carbons, such as graphitized carbon or the incorporation of some promoters to the catalytic system. WO$_x$ promoted electrocatalysts are interesting to evaluate, not only due to its high stability at PEMFC cathode potentials in hydrous, acidic environment and enhanced CO tolerance, but also due to recent reports on introducing WO$_x$-containing materials into different electrodes that have found improved results over similar electrodes with no WO$_x$ content [3-6].

WO$_x$ structures have been reported to perform well as catalyst support in PEMFC cathodes and studies on electrodes, where the Pt has been deposited on C/WO$_x$, showed an increased electrochemically active area of Pt deposited on carbon in the presence of WO$_x$ [7]. Savadogo et. al. [4,5] found that the catalytic activity of 40% WO_3-based electrode was higher than the 10% Pt-based electrode for the ORR. However they found that a mixture of anhydrous WO_3 also increases the electrochemically active surface area of the Pt dispersion on carbon, but the synergistic effect is significantly less than that observed with hydrated WO_3, i.e., tungstic acid. Some other authors have reported that the improvement of fuel cell performance and the increase of the electrochemically active surface area produced by the WO$_s$ incorporation, are caused by synergistic effects between the platinum and oxides materials

---

*To whom correspondence should be addressed: Email: mhernandezp@ipn.mx
Phone: (+) 52 55 57 29 60 00; Fax: (+) 52 55 86 27 28

[6]. Therefore, as the role of the tungsten species is still somewhat debated, in this paper the incorporation of WO_x nanostructures to Pt/C electrocatalysts through different methods was studied in order to determine the influence of the incorporation of WO_x nanostructures over the catalytic activity of Pt/C materials and in the PEMFC cathode stability.

2. EXPERIMENTAL

2.1. Electrocatalysts synthesis

Two Pt-WO_x/C electrocatalysts, and a blank Pt/C sample were prepared using platinum (II) acetylacetonate, $Pt(C_5H_7O_2)_2$, ammonium metatungstate, $(NH_4)_6W_{12}O_{39}\cdot xH_2O)$, and Vulcan XC-72 carbon, with nominal contents: 10 wt. % Pt and 5 wt.% WO_3.

The Pt/C catalyst (*PtC*) was prepared by the photochemical deposition of Pt using a UV-vis lamp of 80 W during 3 h. The procedure of photodeposition method is briefly described as follows. The carbon was dispersed into an ethanol solution of platinum acetylacetonate ($5x10^{-4}$ M), the suspension was ultrasonically irradiated with 25 KHz of power during 15 min at room temperature and stirred vigorously by a magnetic stirrer during 1 h. The suspension was poured into the photo-reactor and the sample was irradiated for 3 h. Finally the product was washed with distilled water several times and dried at 70 °C by about 2 h.

The Pt-WO_x/C samples were prepared by two methods. The catalyst prepared by method I (*PtCW-I*) was prepared by the impregnation of the *PtC* sample with an ethanol solution of ammonium metatungstate ($1x10^{-5}$ M), the solution was stirred by 1 h at room temperature, then NH_4OH was added to reach pH 10. The product was washed repeatedly and then dried at 110 °C for about 2 h. This sample was labeled as *PtCW-I.*

The catalyst prepared by method II was synthesized by coprecipitation of Pt and tungsten and chemical reduction with sodium borohydride ($NaBH_4$). A solution of platinum acetylacetonate, ammonium metatungstate and ethanol was stirred with the respective portion of Vulcan XC-72 carbon during 1 h at room temperature; afterwards NH_4OH was added to reach pH 10. The product was washed repeatedly and then excessive $NaBH_4$ solution was added drop by drop and stirred for 3 h. Finally, the slurry was washed with distillated water, filtered and dried at 110 °C for about 2 h. This catalyst was denoted as *PtCW-II.*

2.2. Electrochemical measurements

A conventional single three-electrode test electrochemical cell was used in the electrochemical experiments. All of the electrode potentials in this work are related to a normal hydrogen electrode (NHE) in a 0.5 M H_2SO_4 aqueous solution electrolyte. The rotating disk electrode (RDE) measurements were performed using a Potentiostat (EG&G PAR 263A) and a Pine MSRX rotation speed controller. All electrochemical experiments were conducted at room temperature. The working electrode was a glassy carbon disk with a 5 mm diameter (0.19 cm^2). Glassy carbon and reference hydrogen electrodes were used as the counter and the reference electrode. The catalytic ink was prepared by dispersing 1 mg of catalyst in 8 μL of Nafion® and 60 μL of ethyl alcohol in an ultrasound bath for 15 min. A drop containing 8 μL of catalyst ink was deposited onto the working electrode surface and dried at atmospheric conditions. Cyclic voltammetry (CV) was used to activate the electrocatalyst. The CV measurements were developed in a nitrogen-saturated electrolyte from 0.0 to 1.2 V (NHE) at 50 mV s^{-1} until a steady-state voltammogram was reached; approximately 10 cycles were necessary.

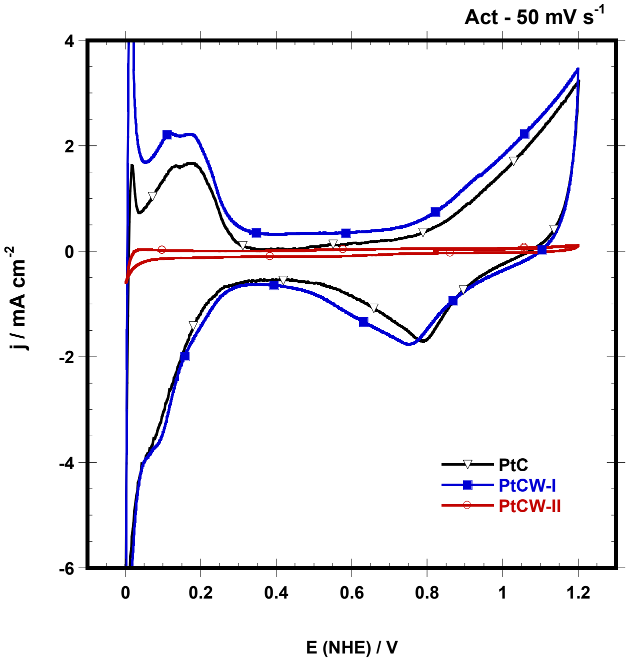

Figure 1. Cyclic voltammetry of PtC, PtCW-I and PtCW-II catalysts in O_2 free 0.5 M H_2SO_4 solution. Scan rate potential of 50 mVs^{-1}.

Steady-state polarization curves were obtained with the RDE at several rotation speeds (100 to 1600 rpm at 5 mV s^{-1}) to evaluate the ORR kinetic parameters, and the experiments were recorded in the potential range between open circuit potential and 0.2 V (NHE) and using the acid electrolyte saturated with pure oxygen and maintained on the electrolyte surface during the RDE tests. The current density was calculated using the geometric surface area.

A stability study, through chronopotentiometry technique for 30 h at 0.78V (NHE), was performed in oxygen atmosphere and rotation speed of 100 rpm over the *PtCW-I* catalyst.

2.3. Physicochemical characterization

The samples were studied in order to analyze morphology and particles distribution using high-resolution transmission electron microscopy (HRTEM). The micrographs were obtained in a TITAN 80-300 with Schottky type field emission gun operating at 300 kV. The point resolution and the information limit were better than 0.085 nm. HRTEM digital images were obtained using a CCD camera and Digital Micrograph Software from GATAN. In order to prepare the materials for observation, the powder samples were ultrasonically dispersed in ethanol and supported on holey carbon coated copper grids. Pt and tungsten dispersion and local contents were studied by SEM using a Nova200 Nanolab, Dual Beam Microscope, Field Emission Scanning Electron Beam, which has 1.1 nm of resolution, and a Focused Ion Beam, with 1.7 nm of resolution.

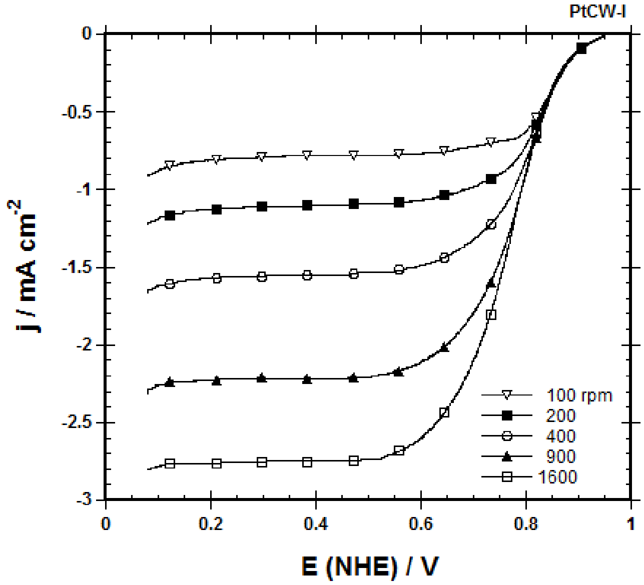

Figure 2. Polarization curves for PtCW-I in O_2 saturated 0.5 M H_2SO_4 at different rotation rates.

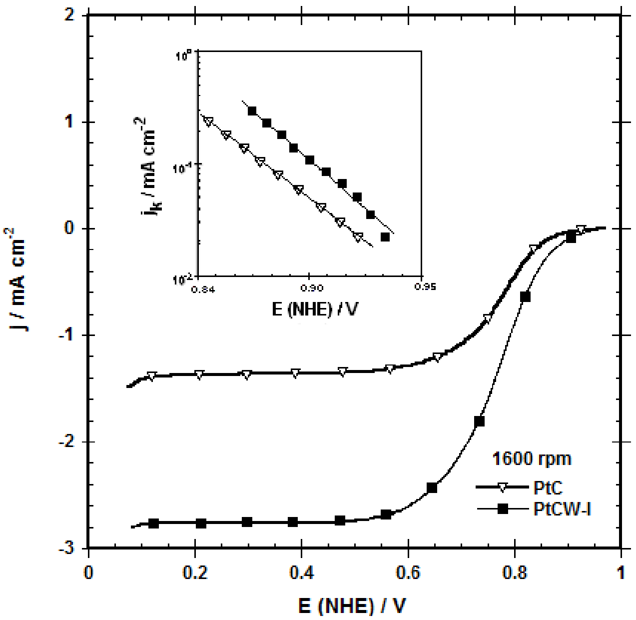

Figure 3. Comparison of the polarization curves in O_2 saturated 0.5 M H_2SO_4 at 1600 rpm and mass transfer corrected Tafel plots for the ORR on PtC and PtCW-I catalysts.

3. RESULTS AND DISCUSSION

The cyclic voltammetry (CV) characterization of the platinum electrode in the supporting electrolyte was performed in a nitrogen purged 0.5 M H_2SO_4 solution, at a 50 mV s^{-1} scan rate. In this experiment, the electrodes were submitted to 10 cycles in order to obtain reproducible voltammograms. Figure 1 presents voltammograms of the three platinum samples for comparison purposes. The PtC and PtCW-I electrodes present good definition in adsorption-desorption hydrogen region, which is characteristic in polycrystalline noble metals. The voltammograms of the PtC and PtCW-I electrodes show similar surface reactions in a potential region of 0.0 V–0.3 V/NHE. Analysis at a more positive potential, corresponding to the anodic region, also shows a well-defined hydroxide-adsorbed peak with a slight difference in the current magnitude, which indicates that both catalysts have a similar capacity for anion adsorption. Cathodic scan shows the same reduction potential of the oxides formed during anodic sweep. The reduction peaks of PtCW show a slight displacement to cathodic potential. The addition of carbon as electron conducting component compensates for the low electronic conductivity of WO$_x$.

On the other hand, the PtCW-II catalyst, Figure 1, shows a striking difference in the current magnitude in all potential scan. The PtCW-II presents an expected low electrochemically active area in the hydrogen region as well as low oxygen reduction activity and a decrease double layer capacitance; it is presumably due to a reduced direct contact between Pt and the reactants, produced by a coating of platinum with tungsten. Then, it is found that is better to synthesize WO$_x$ to the Pt-C than synthesize to the Pt-WO$_x$-C together cathode performance of the composite electrode could be achieved in combination with an improved stability.

The polarization curves on PtCW-I, incorporated into a Nafion® film electrode, were performed at different rotation rates, in an oxygen-saturated 0.5 M H_2SO_4 solution at 25 °C, Figure 2. The polarization curves show three well defined potential zones: charge transfer, mixed and mass transport. It was considered that defined limiting currents are associated with the high diffusion of oxygen through the electrode surface and the uniform distribution of active sites. On the PtCW-I electrocatalyst, the oxygen reduction is fast enough that, at high over-potentials, a flat limiting plateau is observed. This phenomenon can be associated to a good distribution of the electrocatalytic sites on the electrode surfaces. On a film-coated electrode surface, the overall measured density current (j), is related to the kinetic density current (j_k), the boundary layer-layer diffusion-limited density current (j_d), and the film diffusion-limited current (j_f), by equation (1). The effect of the film diffusion is significant only in cases where the electrode is covered by the Nafion film and can be neglected in the present study since the amount of Nafion (0.96 µl 5 wt.% Nafion in 8 µl of solution) in the prepared catalyst suspension is sufficiently small. Hence, it should not be considered a factor in the limiting current density. Thus, the overall measured current of the oxygen reduction can be written as being dependent on the kinetic current and the diffusion-limited current, as shown on the left side of the following equation:

$$\frac{1}{j}=\frac{1}{j_k}+\frac{1}{j_d}+\frac{i}{j_f}=\frac{1}{j_k}+\frac{1}{B\omega^{1/2}} \tag{1}$$

The kinetic current density is proportional to the intrinsic activity of the catalyst. The constant B is $0.2nFCD^{2/3}n^{-1/6}$, where 0.2 is a constant used when ω is expressed in revolutions per minute, C is the bulk concentration of oxygen (1.1×10^{-6} mol cm^{-3}), D is the diffusion coefficient of oxygen in the sulfuric acid solution (1.4×10^{-5} cm^2 s^{-1}), and ν is the kinematic viscosity of the sulfuric acid

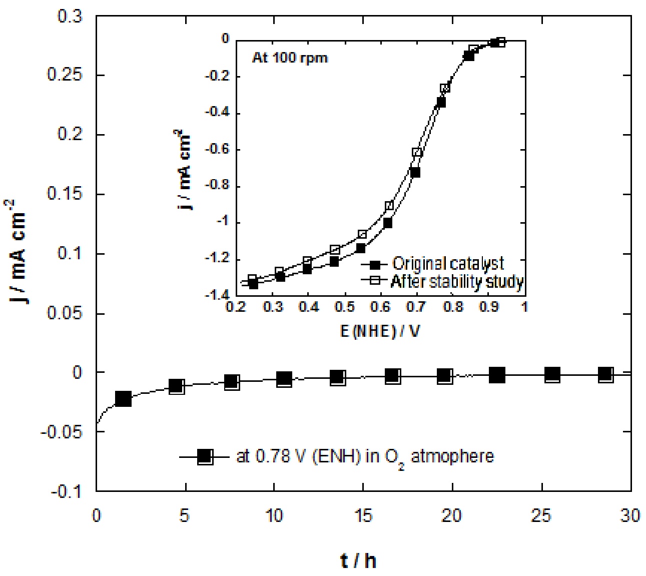

Figure 4. Chronopotentiometry study for 30 h at 0.78V (NHE) in oxygen atmosphere and rotation speed of 100 rpm over the *PtCW-I* catalyst.

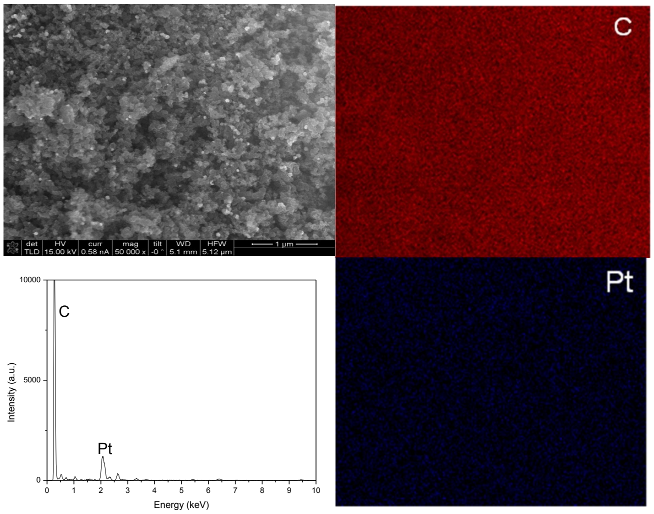

Figure 5a. EDS and Pt and C chemical mapping of the PtC catalyst.

(1.0×10^{-2} cm^{-2} s^{-1}).

Figure 3 displays the ORR activity of PtC and PtCW-I at a rotating speed of 1600 rpm and 25 °C. The PtCW-II electrode showed very low oxygen reduction activity and the response is not included in this figure. As observed in this figure, the ORR, in the activation region is more favorable for the PtCW-I catalyst and the current density is higher than PtC. The inset in Figure 3 shows the mass-transfer-corrected Tafel plots for the PtC and PtCW-I. Tafel slope at low current density show values of 76 mV dec^{-1} and 77 mV dec^{-1} respectively, which indicates that the first electron transfer on the adsorbed oxygen molecule is the rate-determining step. This behavior is in agreement with results reported by other authors for PtC and PtCW-I catalysts prepared by other synthetic methods [8-9]. Table 1 summarizes all the kinetic parameters deduced for the ORR on the PtC and PtCW-I electrocatalysts. Moreover, a stability study through chronopotentiometry technique for 30 h at 0.78V (NHE) was performed in oxygen atmosphere and rotation speed of 100 rpm over the PtCW-I catalyst (Figure 4). The catalyst showed high stability in the reaction medium to ORR during this period of time. In future work we will test Pt-WO_x/C catalysts as cathode in a fuel cell, to determine its performance and stability in real operating conditions.

From Table 1 it is observed the same open circuit potentials to both analyzed samples, 0.97 V. The potentials at a current density of 0.1 mA cm^{-2}, were 0.88 V and 0.90 V to PtC and PtCW-I respectively. Therefore, the electrochemical results indicate that the incorporation of WO_x enhance the catalytic activity towards the ORR.

Figure 5 shows the results from SEM analysis of a) PtC, b) PtCW-I and c) PtCW-II catalysts. EDS and chemical mapping were obtained from different regions of the samples, always showing a homogeneous dispersion of Pt, W, O and C, depending of their chemical composition. It is observed that in PtCW-I and PtCW-II samples, the Pt and W signals are distributed over the entire surface, which indicates that these components are dispersed on the surface. However by TEM higher concentration in preferable zones was observed in the PtCW-II sample, which in part explains the lower performance of this sample. Interestingly, the Pt and W content were lower that the nominal composition considered for the synthesis, due to the formation of platinum or tungsten oxides, from the uniform presence of oxygen over the entire sample.

TEM analysis was carried out on the PtCW-I catalyst to characterize the morphology and size of particles, Figure 6. It is noted that the material has a regular morphology. Pt particles have a uniform size and it is observed that they are uniformly impregnated with mean diameters at about 2-5 nm. The physicochemical results indicate a good dispersion of the Pt and WO_x nanoparticles on the carbon surface produced by the synthesis method I, however it was difficult to identify the structure and coordination of the WO_x species. The tungsten oxide species present in an aqueous solution varies as functions of the pH of the impregnating solution and concentration [10], the equilibrium between monomeric WO_4^{2-} and polymeric $W_{12}O_{42}^{12-}$ species. The tetrahedrally coordinated WO_4^{2-} is the predominant species in basic solution, in this case by adding NH_4OH in a controlled way, we observed the precipitation of a

Table 1. Kinetic parameters deduced from Tafel slope in ORR on PtC and PtCW-I Catalysts.

Muestra	E_{ca} V/ENH	$-b$ mV dec^{-1}	a	j_o mA cm^{-2}	Potential / V j =0.1 mA cm^{-2}
PtC	0.97	77	0.76	2.86×10^{-6}	0.88
PtCW-I	0.97	76	0.77	5.78×10^{-6}	0.90

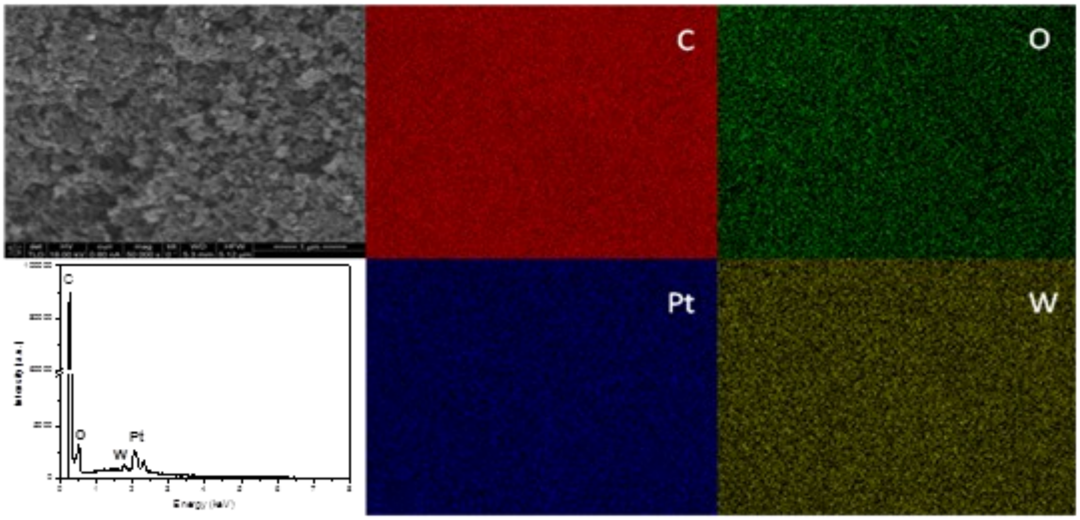

Figure 5b. EDS and Pt, W, O and C chemical mapping of the PtCW-I catalyst.

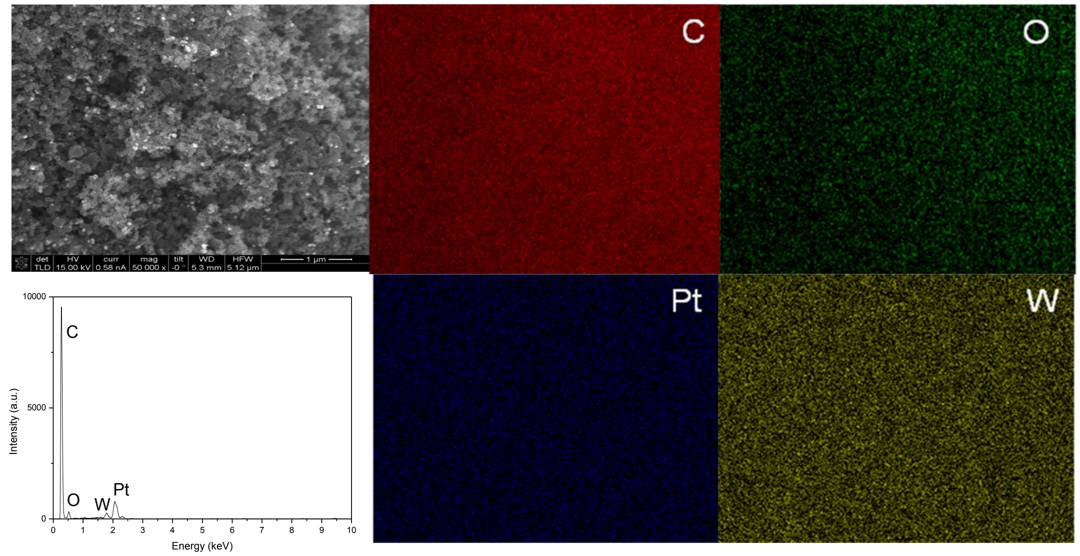

Figure 5c. EDS and Pt, W, O and C chemical mapping of the PtCW-II catalyst.

white gelatinous solid, then it is possible that these monomeric species with tetrahedral coordination interact with the reduced platinum during the precipitation producing a synergetic effect between these species (Method I), however, the coprecipitation of tungsten and platinum precursors decreases the catalytic activity of the Pt/C material, probably due to the tungsten species cover the Pt surface, avoiding the oxygen accessibility to the metallic particle.

4. CONCLUSION

The results indicate that the higher activity of the PtCW-I sample prepared by the deposition of WO_x species on Pt/C generates a higher number of active size on the surface than the simultaneous precipitation of platinum and tungsten, probably due to a higher Pt dispersion along with the synergetic effect of Pt and the WO_x species. This catalyst also showed good stability in the chronopotentiometry study for 30 h. However, further studies about the tungsten composition and crystalline structure, as well as tests of Pt-WO_x/C catalysts as cathode in a fuel cell are needed.

5. ACKNOWLEDGMENTS

Authors would like to acknowledge to the IPN for the grants and financial support received (SIP-20120486, 20120475 and multidisciplinary project SIP-13138), as well as the CONACYT (Project 130254). The authors also acknowledge the facilities of the Electron Microscopy Laboratory of the Instituto Mexicano del Petroleo for this work.

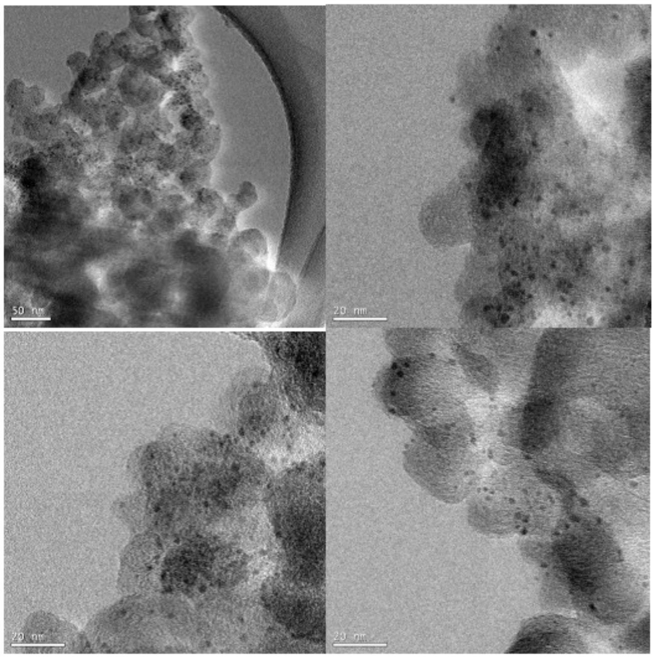

Figure 6. TEM images of the PtCW-I catalyst in different zones.

REFERENCES

[1] L. Timperman, Y.J. Feng, W. Vogel, N. Alonso-Vante, Electrochim. Acta, 55, 7558 (2010).

[2] M.S. Saha, M.N. Banis, Y. Zhang, R. Li, X. Sun, M. Cai , F.T. Wagner, J. Power Sources, 192, 330 (2009).

[3] A.K. Shukla, M.K. Ravikumar, A.S. Arico, G. Candiano, V. Antonucci, N. Giordano, A. Hamnett, J. Appl. Electrochem., 25, 528 (1995).

[4] O. Savadogo, P. Beck, J. Electrochem. Soc., 143, 3842 (1996).

[5] O. Savadogo, A. Essalik, J. Electrochem. Soc., 143, 1814 (1996).

[6] J. Shim, Ch. Lee, H. Lee, J. Lee , E. J. Cairns, J. Power Sources, 102, 172 (2001).

[7] Z. Cui, L. Feng, Ch. Liu , W. Xing, J. Power Sources, 196, 2621 (2011).

[8] Y. Wang, S. Song, V. Maragou, P.K. Shen , P. Tsiakaras, Appl. Catal. B: Environmental, 89, 223 (2009).

[9] E. Antolinia , E.R. Gonzalez, Appl. Catal. B: Environmental, 96, 245 (2010).

[10]D.S. Kim, M. Ostromecki, I.E. Wachs, Catal. Lett., 33, 209 (1995).